Progress In Electromagnetics Research, Vol. 124, 365–381, 2012

A NEW TRI-BAND BANDPASS FILTER FOR GSM, WIMAX AND ULTRA-WIDEBAND RESPONSES BY USING ASYMMETRIC STEPPED IMPEDANCE RESONATORS

W.-Y. Chen[1, *], M.-H. Weng[2], S.-J. Chang[1], H. Kuan[3], and Y.-H. Su[3]

[1]Institute of Microelectronics and Department of Electrical Engineering, Advanced Optoelectronic Technology Center, Center for Micro/Nano Science and Technology, National Cheng Kung University, No. 1, University Rd., East District, Tainan City 701, Taiwan

[2]Medical Devices and Opto-electronics Equipment Department, Metal Industries Research & Development Center, 6F, No. 168, Benzhou Rd., Gangshan, Kaohsiung 820591, Taiwan

[3]Department of Electro-Optical Engineering, Southern Taiwan University, Taiwan, No. 1 Nantai St., Yongkang City, Tainan County 71005, Taiwan

Abstract—In this paper, a design of new tri-band bandpass filter for the application of GSM (1.8 GHz), WiMAX (2.7 GHz) and UWB (3.3–4.8 GHz) is proposed. The first two narrow passbands are created, and the bandwidth of the third passband can be tuned by properly selecting the impedance ratio (R) and physical length ratio (u) of the asymmetric stepped-impedance resonator. To improve passband performance and form the UWB passband, a U-shape defected ground structure and extra extended coupling lines are integrated with the asymmetric SIR. Due to the three transmission zeros appearing near the passband edges, the band selectivity of the proposed filter is much improved. The filter was fabricated, and the measured results have a good agreement with the full-wave simulated ones.

1. INTRODUCTION

In recent years, multiple service technology is widely and aggressively developed, especially in the radio frequency devices of the wireless

Received 20 December 2011, Accepted 13 January 2012, Scheduled 4 February 2012

* Corresponding author: Wei-Yu Chen (mark00.chen@gmail.com).

communication systems. To achieve the requirement in commercial products with multi-service, the circuit with high integration of multi-bands has become more significant. In the radio frequency (RF) front end, the bandpass filter (BPF) plays a key component for selecting the desired and high resolution signals. To design a multiband filter with multiple services is becoming an important issue and carried out in many literatures.

In topologies of filter design, substrate integrated waveguide (SIW), multi-mode ring resonators, stub loaded resonator (SLR) and stepped-impedance resonator (SIR) are widely used to realize the multi-band responses [1–16]. In [1], the tri-band Chebyshev filter and dual-band quasi-elliptic filter with inverter coupling resonator were demonstrated with SIW technology. In [2], a new modal orthogonality of SIW was used to realize a tri-band response with low-loss co-fired ceramic (LTCC) technology. All of the passbands within these two investigations were allocated closely since transmission lines with extremely high impedances could be easily performed as compared to the planar fabrication process. The transmission poles and transmission zeros are achieved by a multi-coupling path in the SIW structure. However, the multi-band filter with UWB response is hard to realize by SIW topology. In [3], the ring-like SIR with embedded coupled open stubs resonators were realize two passbands individually and several transmission zeros aside the passband. In [4], a pair of asymmetric SIRs with cross-coupled arrangement was proposed to achieve the dual-band characteristic with high passbands selectivity. In [5], a folded SIR, modified by adding an inner quasi-lumped SIR stub, is used for a new implementation of dual-band filters. In [6], a dual-band filter using open loop ring resonator and defected SIR was presented. In [7], composite resonators consisting of three split-ring resonators was proposed and designed for the tri-band filter. The coupling characteristic and extraction procedures were well discussed in this investigation. However, six resonators were employed to complete their final designs, causing a large circuit area. In [8], a folded stub loaded resonator and defected ground structure resonator were first proposed for a tri-band bandpass filter. In [9], a Differential Evolution (DE) with strategy adaptation was proposed for the design of tri-band filters. However, the multi-band filter with UWB response is not easily realized.

Many tri-band filters have been realized with the SIRs since their multi-modes property is very popular in realizing multi-band responses [10–18]. Stepped impedance resonator has high design freedom of selecting the length ratio (u) and impedance ratio (R) in the structure to achieve the desired frequencies. However, the

typical SIR has a larger circuit size since it is constructed by two step discontinuities, which also generally results in larger insertion loss due to the radiation from the discontinuities. In [18], a triple-band bandpass filter based on tri-section SIR was proposed to realize compact size with low return loss and wideband characteristic. However, the tri-section SIR also has low external quality factors and design complexity to simultaneously satisfy the requirement of the passbands. Moreover, the resonant behaviors of these two SIRs mentioned above are not as flexible as the asymmetric SIR with one step discontinuity. On the other hand, stepped impedance resonators can also be employed to achieve UWB responses by controlling the resonant frequencies in close and forming a strong coupling aside the resonators [19]. In [20], the radial-UIR/SIR loaded stub resonators were presented for designing UWB filter with a good notched band characteristic. Moreover, the UBW filters were designed by the combination of wide passband and rejected notch-band formed by coupled resonators and DGSs [21–23]. In a previous study [24], we designed a UWB filter by forming the tapped technique with the asymmetric SIR. However, most of the proposed studies only provide the dual-band, tri-band performances and UWB responses individually. The integration with dual-band and UWB characteristics is not proposed yet.

Therefore, we use the same asymmetric SIRs to achieve this challenge since the asymmetric SIR has been designed in succession for the multi-bands and ultra-wide band [24, 25]. Unlike the previous study, we achieve the dual-band and UWB responses with a normal coupling structure. In this paper, we propose a design of a new tri-band filter for two narrow passbands at Global System for Mobile Communications (GSM) of 1.8 GHz and Worldwide Interoperability for Microwave Access (WiMAX) of 2.7 GHz and a wide passband at Ultra Wide Band (UWB) from 3.3 GHz to 4.8 GHz. The design guide is to integrate a dual-band filter with two narrow passbands and filters with a wide passband in succession. This paper is organized as follows. Section 2 characterizes the resonant behavior of the asymmetric resonator. The design graphs for determining the center frequencies of the asymmetric SIR are provided. Section 3 provides the design for dual-band characteristics. Section 4 provides the design for wide band characteristics. Section 5 presents the experimental data compared with the simulated results. Finally, Section 6 draws some brief conclusions.

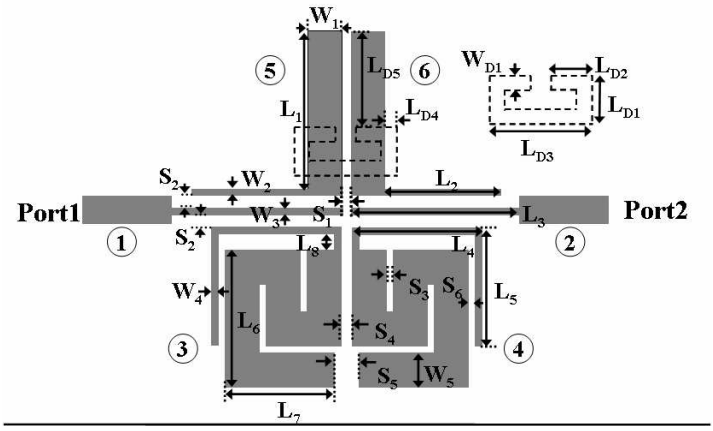

Figure 1. Configuration of the proposed quad-band filter using coupling asymmetric stepped impedance resonators.

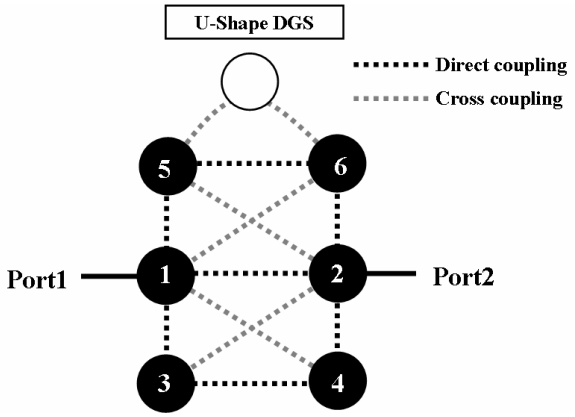

Figure 2. Coupling scheme of the tri-band BPF.

2. DETERMINE THE RESONANCE BEHAVIORS OF ASYMMETRIC SIR

Figure 1 shows the configuration of the proposed filter which can be divided into the upper partition, bottom partition, a pair of feed resonators, and a pair of input/output (I/O) ports. The former consists of a pair of bended asymmetric SIRs and a U-shape DGS, used to form the UWB response, and the latter consists of a pair of asymmetric SIRs, used to form the GSM and WiMAX responses. The coupling

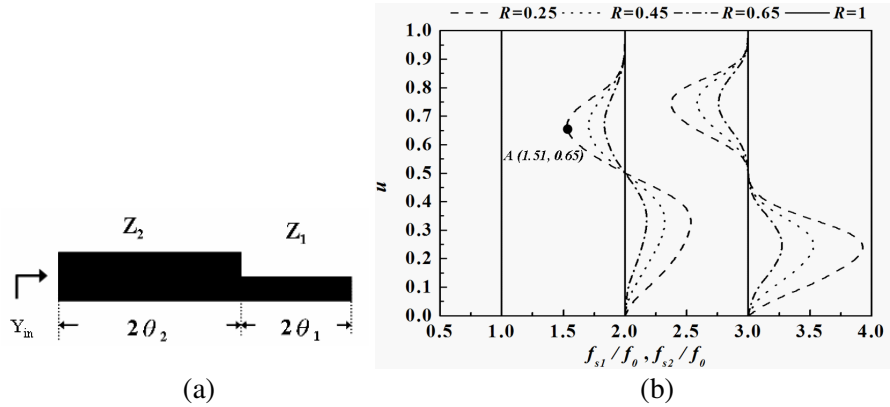

Figure 3. (a) The schematic of asymmetric SIR and (b) normalized resonant behavior of fundamental the higher order resonant frequencies (f_{s1} and f_{s2}) with respect to the fundamental frequency f_0 as function of the length ratio u as the impedance ratio $R = 0.25$, 0.45, 0.65 and 1.

scheme can be figured as Figure 2. The passbands are generated by the direct coupling. Multipath between the input and output can be also observed, which may introduce transmission zeros near the passband response. This proposed tri-band filter was designed and fabricated on Duroid 5880 substrate with a thickness of 0.787 mm, a dielectric constant, ε_r, of 2.2, and a loss tangent of 0.0009.

As shown in Figure 3(a), the structure of asymmetric SIR has only one discontinuity, with a high-impedance section (Z_1) and a low-impedance (Z_2) [24]. It provides the higher external quality factor as compared to the conventional SIR with two discontinuities. To derive the resonant behavior, the input admittance Y_{in} of the proposed asymmetric SIR can be analyzed by the transmission line theory. The $ABCD$ matrix formed by two uniform transmission lines can be expressed as following:

$$A = \cos 2\theta_1 \cos 2\theta_2 - R \sin 2\theta_1 \sin 2\theta_2 \tag{1a}$$

$$B = j(Z_1 \sin 2\theta_1 \cos 2\theta_2 + Z_2 \cos 2\theta_1 \sin 2\theta_2) \tag{1b}$$

$$C = j\left(\frac{\cos 2\theta_1 \sin 2\theta_2}{Z_2} + \frac{\sin 2\theta_1 \cos 2\theta_2}{Z_1}\right) \tag{1c}$$

$$D = \cos 2\theta_1 \cos 2\theta_2 - \frac{\sin 2\theta_1 \sin 2\theta_2}{R} \tag{1d}$$

where the impedance ratio R is generally defined as $R = Z_2/Z_1$, and the $2\theta_1$ and $2\theta_2$ are the electrical lengths of the transmission lines with

characteristic impedances Z_1 and Z_2, respectively. Since the end of the higher impedance line is open circuited, the load impedance at the open end is equal to infinite ($Z_L = \infty$). The input admittance Y_{in} from the end of lower impedance can be regarded as [26]:

$$Y_{in} = \frac{C \cdot Z_L + D}{A \cdot Z_L + B} = \frac{C}{A} \tag{2}$$

The resonant conditions of the asymmetric SIR occurs while $Y_{in} = 0$, and it can be further expressed as:

$$\frac{1 - \tan^2 \theta_1}{\tan \theta_1} = -R \frac{1 - \tan^2 \theta_2}{\tan \theta_2} \tag{3}$$

In order to obtain more design freedom, the length ratio (u) of the asymmetric SIR is also set as a variable and adjusted to achieve the higher order resonant modes. The length ratio (u) is defined as:

$$u = \frac{\theta_2}{\theta_1 + \theta_2} = \frac{\theta_2}{\theta_T} \tag{4}$$

By combining (4) into (3), it can be found that the resonant frequencies of the asymmetric SIR are dependent on length ratio u and impedance ratio R.

It is known that many possible solutions of (u, R) can satisfy the resonant requirement. Figure 3(b) shows the normalized resonant behavior of the fundamental and higher order resonant frequencies, with different length ratios u and impedance ratios $R = 0.25$, 0.45, 0.65. In order to achieve the passbands for GSM of 1.8 GHz and WiMAX of 2.7 GHz (here, $f_{\mathrm{GSM}}/f_{\mathrm{WiMAX}}$ is equal to 1.5), the length ratio u can be explicitly determined as 0.65 for obtaining the dual-band response when considering the asymmetric SIR with $R = 0.25$, as shown in point A of Figure 3. Later, it is noted that in order to simplify the design, we use the same length ratio u and impedance ratio R of the asymmetric SIR for the design of UWB filter.

3. DESIGN OF THE DUAL-BAND CHARACTERISTICS

The specification of the proposed dual-band is set as the center frequency of $f_1 = 1.8$ GHz, and $f_2 = 2.7$ GHz, with fractional bandwidths $\Delta_1 = 3.9\%$ and $\Delta_2 = 2.6\%$, respectively. Based on the design curve of Figure 3(b), the filter structure of the first two narrow passbands, shown in Figure 4(a), consists of the high-impedance ($Z_1 = 156\,\Omega$) line section with a strip width of 0.2 mm and the low-impedance ($Z_2 = 35\,\Omega$) line sections with a strip width of 3.85 mm. The element value of the low-pass prototype filter are $g_0 = 1$, $g_1 = 0.9047$,

$g_2 = 1.2587$, $J_1 = 0.1767$ and $J_2 = 0.7799$ where g_n for $n = 0$ to 2 are the element values and J_n for $n = 1$ to 2 are the admittance inverter constants. Based on the coupling theory according to the standard design procedure given in [26], the coupling matrixes $M_{ij}^{f_1}$ and $M_{ij}^{f_2}$ of the dual-band BPF are derived as follows:

$$M_{ij}^{I} = \begin{bmatrix} 0 & 0.008 & 0.037 & 0 \\ 0.008 & 0 & 0 & 0.037 \\ 0.037 & 0 & 0 & 0.024 \\ 0 & 0.037 & 0.024 & 0 \end{bmatrix} \quad \text{for} \quad 1.8\,\text{GHz} \tag{5}$$

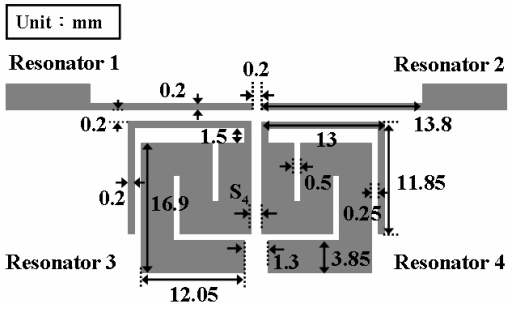

(a)

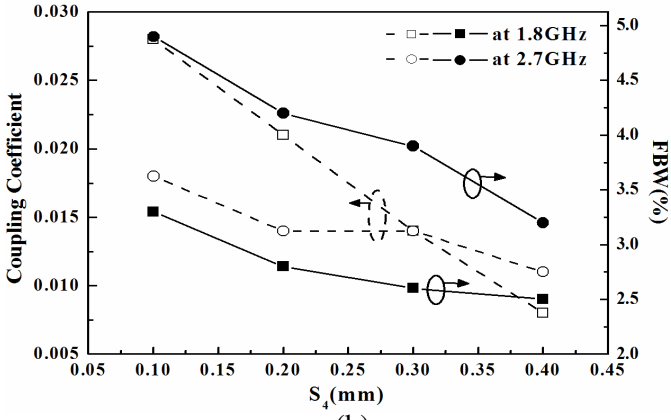

(b)

Figure 4. Coupling coefficients and FBW of first passbands (1.8 GHz) and the second passbands (2.7 GHz).

and

$$M_{ij}^{II} = \begin{bmatrix} 0 & 0.005 & 0.024 & 0 \\ 0.005 & 0 & 0 & 0.024 \\ 0.024 & 0 & 0 & 0.016 \\ 0 & 0.024 & 0.016 & 0 \end{bmatrix} \quad \text{for} \quad 2.7\,\text{GHz} \qquad (6)$$

where M_{ij} is the coupling coefficient of $M_{34} = \text{FBW} \cdot J_2/g_2$, $M_{12} = \text{FBW} \cdot J_1/g_1$ and $M_{13} = M_{24} = \text{FBW}/\sqrt{g_1 g_2}$.

As shown in Figure 4(b), the coupling coefficients and fractional bandwidths with different coupling spacings were calculated by a full-wave EM simulator [27]. Both of the coupling coefficients and fractional bandwidths for the first passband (1.8 GHz) and second passband (2.7 GHz) are as a function of the gap between the two bended asymmetric SIR 3 and SIR 4. It should be noted that the coupling coefficients between the resonator 1 and resonator 2 is very small as compared to SIR 3 and SIR 4, thus the coupling between the resonator 1 and resonator 2 would not affect the characteristics of two passbands as described in [25]. To satisfy the desired fractional bandwidths of the first two passbands, the coupling spacing can be well determined as choosing $S_4 = 0.3$ mm.

Figure 5 shows the magnitude of S_{21} of the two narrow band responses and the phase difference of transmission. It shows that the first passband and second passband are well centered at the desired frequencies of 1.8 GHz and 2.7 GHz with fractional bandwidths of 3.9% and 2.6%, respectively. The three transmission zeros of f_{z1}, f_{z2} and f_{z3} are located at 1.3 GHz, 2.1 GHz and 3.1 GHz. The first two transmission zeros f_{z1} and f_{z2} are a result of the mutli-path coupling effect, which can be easily verified by the phase difference of 180°

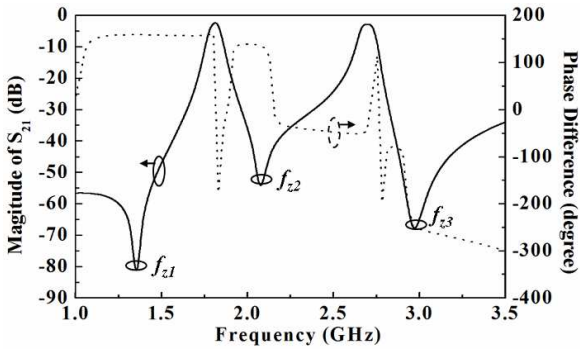

Figure 5. The magnitude of S_{21} of dual band response and the transmission phase difference.

within different transmission paths [8]. The first transmission path is between the resonator 1 and resonator 2, and the second transmission path is the between resonator 3 and resonator 4. It should be noted that the slight inaccuracy of the phase difference of the f_{z2} is due to inter coupling within the bended asymmetric SIRs. The transmission zeros f_{z3} is introduced by the resonator 1 and resonator 2, that is, the resonator 1 and resonator 2 can be seen as an open stub structure while the electromagnetic energy are transmitted by the second transmission path. The introduction of three transmission zeros formed by multi path coupling improves the isolation between the three passbands. The coupling topologies formed by I/O ports, resonator 1, resonant 2 are not easy to achieve the UWB responses, which can be well investigated in the next section.

4. DESIGN OF THE UWB CHARACTERISTICS

The third passband of the proposed filter has an ultra-wide band response. It was reported that to form a UWB response, multi resonant modes shall be coupled together. However, it is hard to form the UWB response by only two resonant modes of the SIRs. Thus, the generation of other modes in the passband is required and important. The compensation technique is required under this case. As proposed in [28], the enhancement of coupling strength formed by DGS was proposed. The DGS is arranged under the resonator 5 and 6 symmetrically to avoid the design complexes and reduction of the compensation. However, the DGS will affect the resonant modes of the asymmetric SIR, thus, the same length ratio u and impedance ratio R, as discussed above, are adapted for the design of ultra-wideband (UWB) response with center frequency near 4.4 GHz to simplify the design. We discuss the property of the DGS first. It was known the DGS under the coupling resonators can be seen as a parallel LC resonator [29]; the capacitance and the inductance can be described as:

$$C = \frac{w_c}{Z_0 g_1} \cdot \frac{1}{w_0^2 - w_c^2} \tag{7a}$$

$$L = \frac{1}{4\pi^2 f_0^2 C} \tag{7b}$$

where w_c is the cut-off frequency of the low-pass filter, Z_0 the scaled impedance level of the in/out terminated ports, and g_1 given by the element value of the prototype low-pass filter. The operating frequency of DGS can be lowered while the reactance is increased by generally increasing the area or the number of DGSs. The design guide of the

proposed third band is to use a pair of asymmetric SIRs for the UWB response and a U-shape DGS formed under the asymmetric SIRs of resonators 5 and 6 to compensate the bandwidth and energy level, as shown in Figure 6(a). Since the impedance ratio R and length ratio u are the same with the design of two other band responses, by shortening the practical length of the SIR 5 and SIR 6, the fundamental modes are firstly designed at 4.4 GHz and 4.65 GHz. However, under this arrangement, it is not easy to achieve the wideband response since two resonant modes are too close and results insufficient bandwidth. Thus, the $1/2\lambda_g$ DGS with the center frequency of 4 GHz is designed, as shown in Figure 6(a) [30]. As shown in Figure 6(b), it can be seen that the two fundamental modes, f_{p1} and f_{p2}, can be adjusted by the

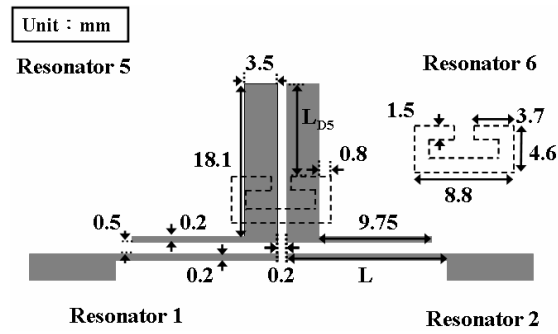

(a)

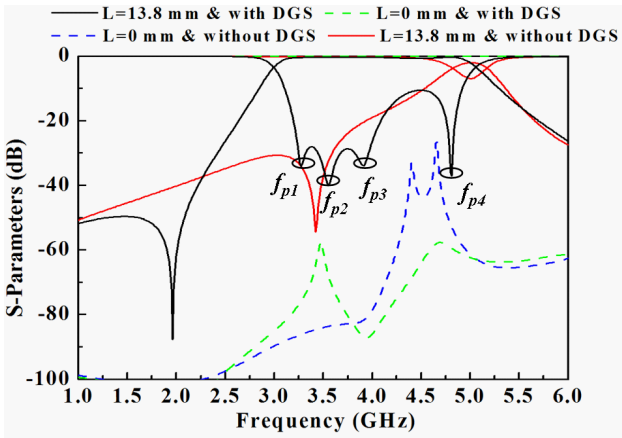

(b)

Figure 6. The UWB frequency response of the three types of the different structure arrangements.

Table 1. Comparison of the tuned length of L with respect to the poles location, bandwidth and max insertion loss.

Length of L (mm)		Poles Locations (GHz)				Bandwidth (GHz)	Max Insertion Loss (dB)
		f_{p1}	f_{p2}	f_{p3}	f_{p4}		
With DGS	$L = 14.8$	3.27	3.52	3.95	4.82	1.95	0.4
	$L = 13.8$	3.25	3.57	3.94	4.82	2.05	0.4
	$L = 13.2$	3.17	3.8	4.05	4.79	2.1	1.2
	$L = 12.6$	3.16	3.88	n/a	4.58	2.2	1.8
	$L = 12$	3.14	3.92	n/a	n/a	2.2	2.2
	$L = 11.4$	3.14	3.95	n/a	n/a	2.3	2.8
	$L = 0$	3.31	4.44	n/a	n/a	n/a	> 20
Without DGS	$L = 13.8$	4.5	4.65	n/a	n/a	0.5	2.1
	$L = 0$	4.4	4.65	n/a	n/a	n/a	> 20

U-shape DGS with the center frequency of 4 GHz. It is found that by lengthening the electrical length of resonator 1 and resonant 2, the first fundamental mode and the second fundamental mode can be further shifted from 4.4 GHz to 3.1 GHz and 4.65 GHz to 3.9 GHz, respectively. Moreover, by adjusting the coupling length of the resonator 1 and resonator 2, another two modes indicated as f_{p3} and f_{p4} are generated within the passband. Table 1 summarized the simulated comparison of the tuned length of L with respect to the poles location, bandwidth and max insertion loss. It is found that the extended coupling length of the resonator 1 and resonator 2 significantly affect the UWB characteristic. It is shown when the coupling line (L) are increased from 0 mm to 13.8 mm and with DGS, the extended coupling provides more electromagnetic level and improves the insertion loss about 14 dB, and thus the UWB response with low insertion loss and desired fractional bandwidth is obtained.

Figure 7 shows the current distributions of the proposed filter operated at 1.8, 2.7, and 4 GHz, respectively. In plots, we can further verify that the electromagnetic waves are transmitted in the designed paths of the filter from port 1 to port 2. It is found in this study each passband can be implemented individually, and low insertion loss and good passband selectivity of the each passband can be also well achieved.

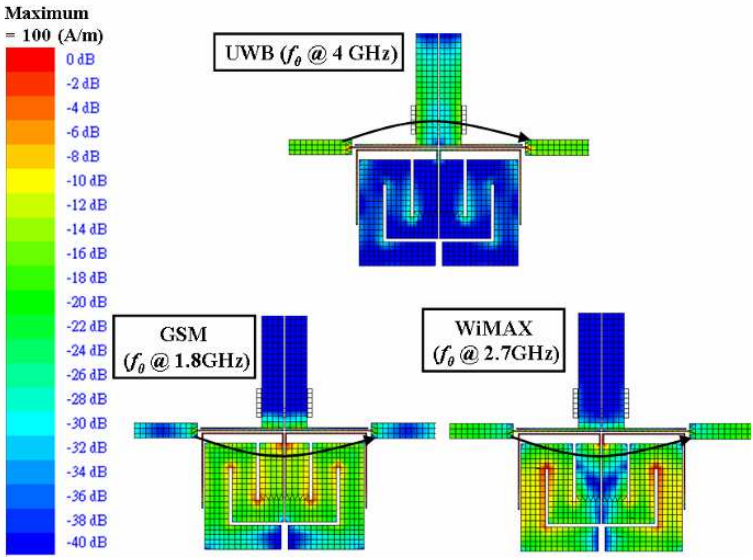

Figure 7. Current distributions of the proposed filter at 1.8, 2.7 and 4 GHz.

5. EXPERIMENTAL RESULTS AND DISCUSSION

The above discussed filter is further tuned and optimized by using the full-wave electromagnetic simulation. The realized parameters are $L_1 = 18.1\,\text{mm}$, $L_2 = 9.75\,\text{mm}$, $L_3 = 13.8\,\text{mm}$, $L_4 = 13\,\text{mm}$, $L_5 = 11.85\,\text{mm}$, $L_6 = 16.9\,\text{mm}$, $L_7 = 12.05\,\text{mm}$, $L_8 = 1.5\,\text{mm}$, $W_1 = 3.5\,\text{mm}$, $W_2 = W_3 = W_4 = 0.2\,\text{mm}$, $W_5 = 3.85\,\text{mm}$, $S_1 = S_2 = 0.2\,\text{mm}$, $S_3 = 0.5\,\text{mm}$, $S_4 = 0.3\,\text{mm}$, $S_5 = 1.3\,\text{mm}$, $S_6 = 0.25\,\text{mm}$, $L_{D1} = 4.6\,\text{mm}$, $L_{D2} = 3.7\,\text{mm}$, $L_{D3} = 8.8\,\text{mm}$, $L_{D4} = 0.8\,\text{mm}$, $L_{D5} = 11.9\,\text{mm}$, and $W_{D1} = 1.5\,\text{mm}$, The full size of the fabricated filter is $37.5 \times 27.8\,\text{mm}^2$, approximately $0.33\lambda_g \times 0.25\lambda_g$, where λ_g means the guided wavelength of the first passband. The photograph of the fabricated BPF is shown in Figure 8(a). The measurement is performed by an Network Analyzer HP 8510C calibrated by the SOLT (Short-Open-Load-Thru) method.

As shown in Figure 8(b), the center frequencies of three passbands are closely matched between the simulated results. The measured results show that the $|S_{21}|$ is greater than $-2.2\,\text{dB}$, $|S_{11}|$ less than $-20\,\text{dB}$, and a fractional bandwidth of 4% for 1.8 GHz, that $|S_{21}|$ is greater than $-2.1\,\text{dB}$, $|S_{11}|$ about $-15\,\text{dB}$, and a fractional bandwidth of 2.8% for 2.7 GHz, and that $|S_{21}|$ is greater than $-1.3\,\text{dB}$, average

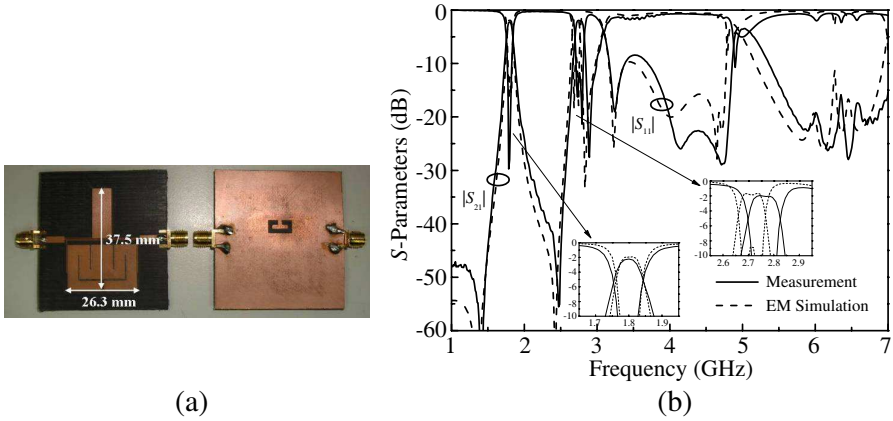

Figure 8. (a) Photograph of fabricated sample. (b) Simulated and measured frequency responses of the fabricated filter.

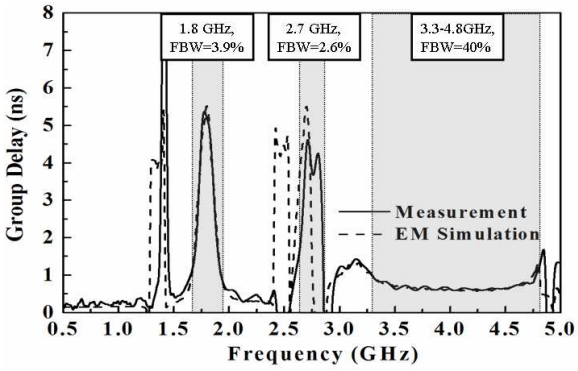

Figure 9. Simulated and measured group delay of the tri-band BPF.

$|S_{11}|$ greater than -15 dB, and a fractional bandwidth of 40% for UWB response. Moreover, it is clearly found that the transmission zeros are located at 1.4 GHz, 2.5 GHz and 2.9 GHz near the passband edges. The appearance of the transmission zeros much improves the selectivity of the proposed filter. Therefore, both isolation levels are around 25 dB between the three passbands. The group delay obtained by taking the derivative of the phase is shown in Figure 9 and varies between 3.7–4.2 ns at 1.8 GHz passband, between 4.6–4.9 ns at 2.7 GHz and between 0.65–1.25 ns at the 3.3–4.8 passband. The filter group delay is inversely proportional to filter bandwidth. In this design, the group delay of the UWB band in the proposed filter is good and satisfied,

Table 2. Comparisons with other proposed tri-band BPF. (FBW: fractional bandwidth).

	1st/2nd/3rd Passband (GHz)	$\|S_{21}\|$ **(dB)**	$\|S_{11}\|$ **(dB)**	**FBW (%)**	**Application**
Ref. [7]	2.4/3.5/5.2	0.9/1.7/2.1	23/15/13	13.5/7/3.5	WLAN WiMAX WLAN
Ref. [15]	2.45/3.5/5.25	2/2.4/1.7	18/16/13	2.5/1.7/5	WLAN WiMAX WLAN
Ref. [16]	2.4/3.8/5.7	0.8/2.0/2.5	22/18/28	7.5/3/4	WLAN WiMAX WLAN
This work	**1.8/2.7/3.3–4.8**	**2.2/2.1/1.3**	**14/13/9**	**3.9/2.6/40**	**GSM WiMAX UWB**

which is not affected by the other two narrow passbands. A slight mismatch between the simulated and measured results, especially for the second passband with 1.8% frequency shift, might be due to the fabrication errors or the variation of material properties. We compared the proposed filter with other reported tri-band filters [7, 15, 16], as summarized in Table 2. First, it is noted that our filter is the first tri-band design having two narrow bands and a UWB band. The insertion loss, band selectivity, as well as the circuit size are all comparative with other design.

6. CONCLUSIONS

A new tri-band bandpass filter using four asymmetric stepped impedance resonators (SIRs) and a U-shape DGS was proposed for the application of GSM (1.8 GHz), WiMAX (2.7 GHz) and UWB (3.3–4.8 GHz). Tri-band response is decided by suitably choosing the impedance ratio (R) and length ratio (u) of the asymmetric SIR and the arrangement of the coupling asymmetric SIRs with the U-shape DGS to satisfy required responses for two narrow bands and ultra-wideband responses, with fractional bandwidths of 4%, 2.8% and 40%, respectively. Three transmission zeros are created near the passband edges, causing a high isolation of 25 dB between the passbands to improve the band selectivity. The measured results show a good

agreement with simulation ones. The proposed filter demonstrating compact size, low insertion loss and good passband selectivity is verified.

REFERENCES

1. Chen, X. P., K. Wu, and Z. L. Li, "Dual-band and triple-band substrate integrated waveguide filters with chebyshev and quasi-elliptic responses," *IEEE Trans. Microw. Theory Tech.*, Vol. 55, 2569–2578, 2007.
2. Tsai, W. L. and R. B. Wu, "Tri-band filter design using substrate integrated waveguide resonators in LTCC," *IEEE MTT-S Int. Microw. Symp. Dig.*, 2011.
3. Chen, W.-Y., M.-H. Weng, S.-J. Chang, and H. Kuan, "A high selectivity dual-band filter using ring-like SIR with embedded coupled open stubs resonators," *Journal of Electromagnetic Waves and Applications*, Vol. 25, Nos. 14–15, 2011–2021, 2011.
4. Weng, M.-H., C.-H. Kao, and Y.-C. Chang, "A compact dual-band bandpass filter with high band selectivity using cross-coupled asymmetric SIRs for WLANs," *Journal of Electromagnetic Waves and Applications*, Vol. 24, No. 2–3, 161–168, 2011.
5. Velazquez-Ahumada, M. D. C., J. Martel-Villagr, F. Medina, and F. Mesa, "Application of stub loaded folded stepped impedance resonators to dual band filters," *Progress In Electromagnetics Research*, Vol. 102, 107–124, 2010.
6. Lai, X., N. Wang, B. Wu, and C.-H. Liang, "Design of dual-band filter based on OLRR and DSIR," *Journal of Electromagnetic Waves and Applications*, Vol. 24, No. 2–3, 209–218, 2010.
7. Luo, S., L. Zhu, and S. Sun, "Compact dual-mode triple-band bandpass filters using three pairs of degenerate modes in a ring resonator," *IEEE Trans. Microw. Theory Tech.*, Vol. 59, 1222–1229, 2011.
8. Lai, X., C. H. Liang, H. Di, and B. Wu, "Design of tri-band filter based on stub loaded resonator and DGS resonator," *IEEE Microw. Wireless Compon. Lett.*, Vol. 20, 265–267, 2010.
9. Liu, Y., W.-B. Dou, and Y.-J. Zhao, "A tri-band bandpass filter realized using tri-mode T-shape branches," *Progress In Electromagnetics Research*, Vol. 105, 425–444, 2010.
10. Lee, C. H., C. I. G. Hsu, and H. K. Jhuang, "Design of a new tri-band microstrip BPF using combined quarter-wavelength SIRs," *IEEE Microw. Wireless Compon. Lett.*, Vol. 16, 594–596, 2006.

11. Hsu, C. I. G., C. H. Lee, and Y. H. Hsieh, "Tri-band bandpass filter with sharp passband skirts designed using tri-section SIRs," *IEEE Microw. Wireless Compon. Lett.*, Vol. 18, 19–21, 2008.
12. Mo, S.-G., Z.-Y. Yu, and L. Zhang, "Design of triple-mode bandpass filter using improved hexagonal loop resonator," *Progress In Electromagnetics Research*, Vol. 96, 117–125, 2009.
13. Zhang, L., Z.-Y. Yu, and S.-G. Mo, "Novel planar multimode bandpass flters with radial-line stubs," *Progress In Electromagnetics Research*, Vol. 101, 33–42, 2010.
14. Chiou, Y.-C. and J.-T. Kuo, "Planar multiband bandpass filter with multimode stepped-impedance resonators," *Progress In Electromagnetics Research*, Vol. 114, 129–144, 2011.
15. Chen, F. C. and Q. X. Chu, "Design of compact tri-band bandpass filters using assembled resonators," *IEEE Trans. Microw. Theory Tech.*, Vol. 57, 165–171, 2009.
16. Guan, X., Z. Ma, and P. Cai, "A novel triple-band microstrip bandpass filter for wireless communication," *Microw. Opt. Tech. Lett.*, Vol. 51, 1568–1569, 2009.
17. Chen, W. Y., Y. H. Su, H. Kuan, and S. J. Chang, "Simple method to design a tri-band bandpass filter using asymmetric SIRs for GSM, WiMAX, and WLAN applications," *Microw. Opt. Tech. Lett.*, Vol. 53, 1573–1576, 2011.
18. Hu, J. P., G. H. Li, H. P. Hu, and H. Zang, "A new wideband triple-band filter using SIR," *Journal of Electromagnetic Waves and Applications*, Vol. 25, No. 16, 2287–2295, 2011.
19. Li, R. and L. Zhu, "Compact UWB bandpass filter using stub-loaded multiple-mode resonator," *IEEE Microw. Wireless Compon. Lett.*, Vol. 17, 40–42, 2007.
20. Liu, C.-Y., T. Jiang, and Y.-S. Li, "A novel UWB filter with notch-band characteristic using radial-UIR/SIR loaded stub resonators," *Journal of Electromagnetic Waves and Applications*, Vol. 25, No. 2–3, 233–245, 2011.
21. Wei, F., L. Chen, Q.-Y. Wu, X.-W. Shi, and C.-J. Gao, "Compact UWB bandpass filter with narrow notch-band and wide stop-band," *Journal of Electromagnetic Waves and Applications*, Vol. 24, No. 7, 911–920, 2010.
22. Xu, J., B. Li, H. Wang, C. Miao, and W. Wu, "Compact UWB bandpass filter with multiple ultra narrow notched bands," *Journal of Electromagnetic Waves and Applications*, Vol. 25, No. 7, 987–998, 2011.

23. Fallahzadeh, S. and M. Tayarani, "New microstrip UWB bandpass filter using defected microstrip structures," *Journal of Electromagnetic Waves and Applications*, Vol. 24, No. 7, 893–902, 2010.
24. Chang, Y. C., C. H. Kao, M. H. Weng, and R. Y. Yang, "Design of the compact wideband bandpass filter with low loss, high selectivity and wide stopband," *IEEE Microw. Wireless Compon. Lett.*, Vol. 18, 770–772, 2008.
25. Chang, Y. C., C. H. Kao, M. H. Weng, and R. Y. Yang, "Design of the compact dual-band bandpass filter with high isolation for GPS/WLAN applications," *IEEE Microw. Wireless Compon. Lett.*, Vol. 19, 780–782, 2009.
26. Hong, J. S., *Microstrip Filters for RF/Microwave Applications*, 2nd Edition, John & Wiley, New York, 2011.
27. *IE3D Simulator*, Zeland Software, Inc., 2002.
28. Zhu, L., H. Bu, and K. Wu, "Aperture compensation technique for innovative design of ultra-broadband microstrip bandpass filter," *IEEE MTT-S Int. Microw. Symp. Dig.*, 2000.
29. Ahn, D., J. S. Park, C. S. Kim, J. Kim, Y. Qian, and T. Itoh, "A design of the low-pass filter using the novel microstrip defected ground structure," *IEEE Microw. Theory Tech.*, Vol. 49, 86–93, 2001.
30. Thomson, N. and J. S. Hong, "Compact ultra-wideband microstrip/coplanar waveguide bandpass filter," *IEEE Microw. Wireless Compon. Lett.*, Vol. 17, 184–186, 2007.